Journal Pre-proof

Transparent, intrinsically fire-safe yet impact-resistant poly(carbonates-b-siloxanes) containing Schiff-base and naphthalene-sulfonate

Ting Sai , Xiaodi Ye , Bingtao Wang , Zhenghong Guo , Juan Li , Zhengping Fang , Siqi Huo

PII: S1005-0302(24)01098-3
DOI: https://doi.org/10.1016/j.jmst.2024.11.023
Reference: JMST 6232

To appear in: *Journal of Materials Science & Technology*

Received date: 30 October 2024
Revised date: 17 November 2024
Accepted date: 26 November 2024

Please cite this article as: Ting Sai , Xiaodi Ye , Bingtao Wang , Zhenghong Guo , Juan Li , Zhengping Fang , Siqi Huo , Transparent, intrinsically fire-safe yet impact-resistant poly(carbonates-b-siloxanes) containing Schiff-base and naphthalene-sulfonate, *Journal of Materials Science & Technology* (2024), doi: https://doi.org/10.1016/j.jmst.2024.11.023

Highlights:

- Poly(carbonates-b-siloxanes) with Schiff-base and naphthalene-sulfonate was developed;
- SS-co-PC9 achieved a UL-94 V-0 rating under a thickness of only 1.6 mm;
- SS-co-PC9 showed a 48% increase in elongation at break compared to pure PC;
- SS-co-PC9 featured high transparency.

Research Article

Transparent, intrinsically fire-safe yet impact-resistant poly(carbonates-*b*-siloxanes) containing Schiff-base and naphthalene-sulfonate

Ting Sai [a, 1], Xiaodi Ye [a, b, 1], Bingtao Wang [a], Zhenghong Guo [a, *], Juan Li [a], Zhengping Fang [a], Siqi Huo [c, *]

[a] Institute of Fire Safety Materials, School of Materials Science and Technology, NingboTech University, Ningbo 315100, China

[b] School of Materials Science and Engineering, Zhejiang Sci-Tech University, Hangzhou 310018, China

[c] Centre for Future Materials, School of Engineering, University of Southern Queensland, Springfield 4300, Australia

[1] These authors contributed equally to this work.

* Corresponding authors.

E-mail addresses: guozhenghong@nbt.edu.cn (Z.H. Guo); Siqi.Huo@unisq.edu.au, sqhuo@hotmail.com (S.Q. Huo).

Abstract

A series of transparent, intrinsically flame-retardant, and impact-resistant poly(carbonates-*b*-siloxanes) were synthesized by incorporating Schiff-base modified polysiloxanes (DMS-Schiff) and naphthalene-sulfonate units into the polycarbonate (PC) chain. In addition to high transparency, the resultant copolymers (SS-co-PC5, SS-co-PC9, SS-co-PC14, and SS-co-PC20) exhibited remarkable improvements in fire safety and mechanical performance. Compared to pure PC, these copolymers demonstrated significantly enhanced limiting oxygen index (LOI, up to 34.5%) and a UL-94 V-0 rating under a thickness of only 1.6 mm. The incorporation of the polysiloxane blocks not only improved flame retardancy but also enhanced the impact strength,

with SS-co-PC9 showing a 48% increase in elongation at break and a 38% rise in impact toughness compared to pure PC. In addition, SS-co-PC9 presented high mechanical strength. The synergistic effects between the naphthalene-sulfonate and polysiloxane blocks, along with the well-controlled polysiloxane phase separation (sulfonate units enabled lower processing viscosity of copolymers), led to superior comprehensive performance. These findings provide a promising pathway to create high-performance copolycarbonates for real-world applications.

Keywords: Polycarbonate copolymer, Microphase separation, Fire safety, Transparency, Impact resistance

1. Introduction

Polycarbonate (PC), particularly bisphenol A-typed PC (BPA-PC), is renowned for its comprehensive performance and stands out from five major engineering plastics for its high transparency [1]. Beyond that, there is an ongoing demand for advanced PC in high-end sectors [2,3], such as 5G communications, aircraft, high-speed trains, smart sensing, optical components, high-impact protection, and medical devices. These sectors face significant demand gaps and supply risks, making an urgent need for the research and development of advanced copolycarbonate (co-PC) to meet the stringent needs [4].

Although PC has an inherent charring capacity, with a limiting oxygen index (LOI) of ~23% and a UL-94 V-2 rating [5], its fire retardancy still cannot satisfy the requirements of the aforementioned high-end sectors. In addition to flame retardancy, there are also strict requirements for smoke suppression and anti-dripping ability, along with the need to achieve excellent mechanical properties, particularly impact resistance, and high transparency under some circumstances [6–8]. Nowadays, the fire-retardant PC is predominantly produced by blending with flame retardants (FRs), such as halides, sulfonates, phosphorus, siloxanes,

nanomaterials, and synergistic systems [9–11]. However, additive FRs suffer from inevitable drawbacks, e.g., poor durability, non-uniform distribution, impairing PC's inherent properties, bioaccumulation, and potential toxicity, making them increasingly inadequate in meeting industrial and environmental requirements [12–14]. Among FRs, sulfonates (a specific FR for PC with an extremely low addition of 0.8–5‰, with minimal impacts on transparency and toughness) [15] and siloxanes (a green FR with both smoke-suppressive and toughening effects towards PC) [16] are particularly promising for meeting the stringent and challenging demands for low-smoke, fire-retardant, impact-resistant, and transparent applications. Notably, they have been reported to have synergistic flame-retardant and anti-dripping effects in PC [17]. However, as additive FRs, sulfonates exhibit disadvantages such as poor dispersibility, and insufficient anti-dripping performance and siloxanes show issues, e.g., a high loading level and poor flowability in the matrix [18, 19].

Consequently, intrinsic flame retardancy offers an effective solution, imposing higher demands on monomer/block synthesis and copolymerization control. Intrinsic flame retardancy can be achieved in thermoplastics, such as polyesters, polyurethanes, and polyamides, by the copolymerization of fire-retardant units, and some commercial products are available [20–22]. Recent reports have proposed strategies for the formation of a dense char without flame-retardant elements during combustion (e.g., ionomer, thermal crosslinking, or rearranged structural units in macromolecules) [13, 23–26]. However, there are few reports on intrinsically flame-retardant PC. For instance, Liaw et al. [27] achieved a 30 °C increase in initial thermal decomposition temperature and a significant LOI improvement (from 25% to 93%) by partially substituting BPA with tetrabromobisphenol A, although transparency and toughness were compromised. Besides, WEEE [28] and RoHS [29] regulations restrict the use of brominated FRs in polymers.

Kambour et al. [30] synthesized a series of co-PCs containing polydimethylsiloxane (PDMS), with enhanced flame retardancy compared to pure PC. Nodera et al. [31] prepared PC-PDMS copolymers, achieving desirable LOI values with the PDMS content of 1%, and Kim's group [32,33] and Nelissen's group [34] reported that small amounts of PDMS in PC copolymers could effectively enhance the film-forming ability and transparency. Chen et al. [35] synthesized macromolecular oligomers containing sulfonate and carbonate, which could be used as additive FRs for PC. Xiao et al. [4] utilized high dissociation energy monomers (dissociation energy: 139.5 kJ mol^{-1}, higher than the conventional BPA monomer) and siloxane to prepare a flame-retardant, thermal-resistant, and closed-loop recyclable co-PCs, maintaining excellent properties after depolymerization and re-polymerization.

Given the high value-added properties, the siloxane copolymerized PC has progressed rapidly in industry. SABIC has commercialized various grades such as EXL, HFD, CXT, and FST, with each targeting specific properties like low-temperature impact resistance, high toughness and flow, flame retardancy, and low smoke release. Samyang and LG Chemical also have related commercial products. Similarly, in China, Wanhua Chemical (STC 3711, 3620, 1221), Cangzhou Dahua (continuous production line), and Gansu Yinguang Group (*Siloxane-co-Polycarbonate Standard*) have filled gaps in the high-end PC field. However, common challenges persist: (i) Thin-walled PC products struggle to achieve a UL-94 V-0 rating. (ii) The content and domain size of siloxane blocks are high (poor microphase separation), affecting the transparency of co-PC. (iii) The structure-property relationship of co-PC is unrevealed. These deficiencies hinder the development of fire-retardant and smoke-suppressive co-PC with anti-dripping performance and result in a failure to provide a sufficient theoretical basis for performance optimization.

Herein, we applied sulfonates as efficient flame-retardant units and siloxanes as impact-resistant and smoke-suppressing blocks for PC to fabricate transparent, intrinsically flame- and impact-resistant poly(carbonates-*b*-siloxanes). Moreover, a structure-performance relationship was established, thereby providing a theoretical foundation and new approach for the development of high-value-added flame-retardant copolycarbonates.

2. Experimental section

2.1. Materials

Octamethylcyclotetrasiloxane (D4, ≥ 98%), 3-aminopropylmethyldiethoxysilane (APS, ≥ 97%), benzaldehyde (≥ 99%), bisphenol A (BPA, ≥ 99%), diphenyl carbonate (DPC, ≥ 99%), and disodium 2,7-dihydroxynaphthalene-3,6-disulfonate (DN-SO_3Na, ≥ 98%) were purchased from Aladdin (Shanghai, China). 5,5-dimethyl-1-pyrroline-N-oxide (DMPO, as a spin trapping agent, ≥ 99%), tetrabutylammonium hydroxide (TBA, ≥ 99%, specific roles as a catalyst are pH adjustment, reaction rates promotion, and surface tension reduction), and tetramethylammonium hydroxide pentahydrate ($Me_4NOH{\cdot}5H_2O$, ≥ 97%) were provided by Sigma-Aldrich (U.S.). Dimethyl sulfoxide (DMSO, ≥ 99%), tetrahydrofuran (THF, ≥ 99%), dichloromethane (CH_2Cl_2, ≥ 99%), ethanol (≥ 99%), and N,N'-dimethylformamide (DMF, ≥ 99%) were purchased from Sinopharm Reagent (Shanghai, China). Chloroform-d_6 ($CDCl_3$) ≥ 99.8%) was obtained from Macklin (Shanghai, China). Deionized water (H_2O) was prepared by our laboratory.

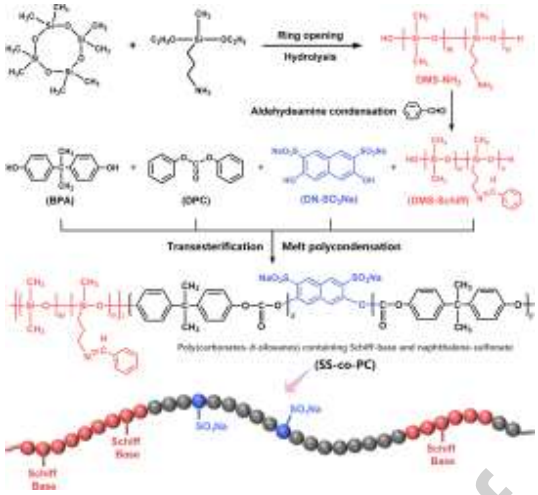

Fig. 1. Synthesis of Schiff-base modified polysiloxanes (DMS-Schiff) and poly(carbonates-*b*-siloxanes) (SS-co-PC).

2.2. Synthesis of Schiff-base modified polysiloxanes (DMS-Schiff)

As shown in Fig. 1, $Me_4NOH{\cdot}5H_2O$ (2.3 g, 0.01 mol) as a catalyst, DMSO (5.4 g, 0.07 mol), D4 (59.3 g, 0.20 mol), APS (17.2 g, 0.09 mol) and H_2O (5 mL) were introduced into a flask and stirred at 80 °C for 4 h to achieve ring-opening and hydrolysis. Ethanol generated during this process was removed by vacuum distillation. The preliminary product was subsequently stirred at 110 °C for 24 h to increase the molecular weight via polycondensation. Then, the residual catalyst, solvent, and impurities were removed completely at 190 °C, yielding amino-containing polysiloxanes (noted as DMS-NH_2). The obtained DMS-NH_2 (60.0 g, ~0.005 mol) and benzaldehyde (1.1 g, 0.01 mol) were dissolved in 30 mL of THF and heated to 70 °C and stirred for 20 h to complete the aldehyde-amine condensation. After removing the solvent under vacuum, the Schiff-base modified polysiloxanes (noted as DMS-Schiff) were obtained.

2.3. Preparation of poly(carbonates-b-siloxanes) (SS-co-PC)

Copolycarbonates were named SS-co-PC5/9/14/20, in which the numbers indicate the polysiloxane block content of copolymer based on ^{13}C nuclear magnetic resonance (^{13}C-NMR)

spectra. Typically, BPA (22.8 g, 0.1 mol), DPC (42.8 g, 0.2 mol), DN-SO_3Na (0.054 g, 0.15 mmol), DMS-Schiff (53.5 g, 0.005 mol) and TBA (catalyst, ~10^{-3} mmol, specific roles for pH stabilization, enhancing positive reaction rates and yields, and surface tension reduction) were added into a reactor (Fig. 1). Under argon atmosphere to prevent oxidative degradation, the transesterification was carried out for 6 h at 180 °C. The reactor pressure was reduced to 125 Pa to continuously remove byproducts such as alcohol and volatile impurities via vacuum distillation, and then the system was heated to 260 °C for 30 min to thoroughly achieve polycondensation. Finally, the mixture was cooled to room temperature, dissolved in CH_2Cl_2, and then precipitated as a solid with ethanol. The precipitated copolycarbonate was collected by filtration and washed thoroughly with ethanol to remove any residual solvent or impurities. After filtration, the crude product was dried at 100 °C for 7 h to obtain SS-co-PC5. When the addition amount of DMS-Schiff was shifted as 0.10, 0.15, and 0.20 mol, SS-co-PC9, SS-co-PC14, and SS-co-PC20 were obtained, respectively.

SS-co-PCs were dried in an oven at 80 °C for 20 h to thoroughly remove residual moisture or solvents. The copolymers were then subjected to melt processing in a torque rheometer (ThermoHaake 600, Germany) under 225 °C for 7 min with a rotating speed of 60 rpm. The resultant copolycarbonates were preheated for 6 min and pressed (18 MPa, 230 °C, and 3 min) in molds to fabricate all standard specimens.

2.4. Characterization

This section is included in the Supplementary Information.

3. Results and discussion

3.1. Characterizations of DMS-Schiff and SS-co-PCs

As shown in Fig. 1, the preparation of the hydroxyl-terminated polysiloxane blocks required for the poly(carbonates-*b*-siloxanes) (SS-co-PCs) involved the synthesis of DMS-NH_2 (via ring-opening and hydrolysis reactions) and DMS-Schiff (through an aldehyde-amine condensation under mild conditions). Based on the previous reports [18, 36], in the ^{1}H-NMR spectrum of DMS-NH_2 (Fig. 2(a)), the chemical shifts of protons in amino and adjacent methylene appear at 3.14 and 2.71 ppm, respectively. Additionally, the signals at 1.49 and 0.51 ppm belong to another two adjacent methylene protons, and those (e) and (e') correspond to the protons of methyl bonded to Si directly (two distinct environments). In contrast, the ^{1}H-NMR spectrum of DMS-Schiff displays the disappearance of the amino signals, indicating successful aldehyde-amine condensation. A peak at 8.35 ppm, corresponding to the –N=C–H proton, is observed. The signal of methylene adjacent to the Schiff-base shifts from 2.71 to 3.67 ppm, and multiplet peaks between 7.34 and 8.32 ppm appear, corresponding to protons in aromatic structures. The remaining proton signals are consistent with those of DMS-NH_2.

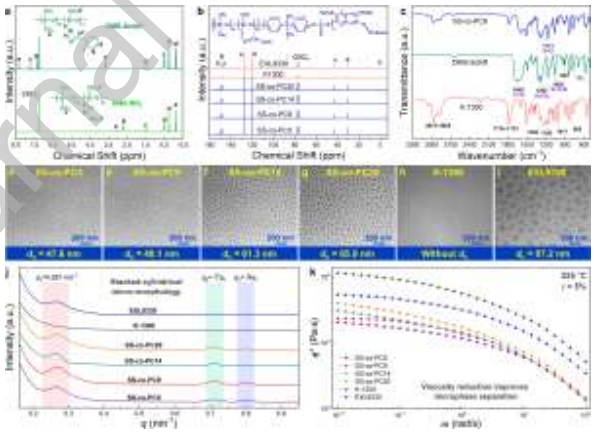

Fig. 2. (a) ^{1}H-NMR spectra of polysiloxane oligomers (DMS-NH_2 and DMS-Schiff). (b) ^{13}C-NMR spectra of SS-co-PCs, K-1300 and EXL9330. (c) FT-IR spectra of DMS-Schiff, SS-co-PC9, and K-1300. (d–i) TEM images, (j) SAXS profiles, and (k) complex viscosity (η^*) versus frequency (ω) curves of SS-co-PCs, K-1300 and EXL9330.

The Fourier transform infrared (FT-IR) spectra in Fig. 2(c) further confirm the formation of DMS-Schiff. The absorption bands at 1062 and 771 cm^{-1} can be attributed to the stretching vibrations and fingerprint region peaks of the Si–O–Si group. The peaks at 1268 and 903 cm^{-1} correspond to the stretching and out-of-plane deformation vibrations of $Si\text{-}CH_3$, respectively. Notably, the stretching vibration of the C=N bond appears at 1649 cm^{-1}, corroborating the findings in ^{1}H-NMR. These results confirm the successful synthesis of DMS-NH_2 and DMS-Schiff. As summarized in Table 1, the molecular weight and distribution of DMS-Schiff were further analyzed using gel permeation chromatography (GPC), with DMF as a solvent. The number-average and weight-average molecular weights (M_n and M_w) of DMS-Schiff were 1.07×10^4 and 1.88×10^4 g mol^{-1}, respectively, with a polydispersity index (PDI) of approximately 1.76. This is comparable to the narrow distributions of polydimethylsiloxanes reported in the literature [37].

Table 1 The block and elemental content, molecular weight (M_n, M_w), and its polydispersity index (PDI) of DMS-Schiff, SS-co-PCs, and commercial grades. (The reasonably increased polysiloxane content brings about the remarkably improved toughness and smoke suppression of SS-co-PCs but has little effect on transparency and tensile strength. The introduction of sulfonate units reduces the processing viscosity of SS-co-PCs, thus promoting the microphase separation.)

Sample ID	[a] Polysiloxane block content (%)	[b] S content (%)	M_n (g mol^{-1})	M_w (g mol^{-1})	PDI	Yield (%)
DMS-Schiff	–	–	1.07×10^4	1.88×10^4	1.76	93
SS-co-PC5	5.02	0.020	1.70×10^4	6.02×10^4	3.54	85
SS-co-PC9	9.26	0.018	1.82×10^4	6.29×10^4	3.46	85
SS-co-PC14	14.31	0.015	2.07×10^4	6.65×10^4	3.21	82
SS-co-PC20	20.28	0.011	2.18×10^4	6.69×10^4	3.07	82
[c] K-1300	0.00	–	1.80×10^4	3.36×10^4	1.87	–
[d] EXL9330	11.27	–	1.68×10^4	5.01×10^4	2.98	–

[a] Calculated by the integral areas in ^{13}C-NMR spectra (Fig. 2(b)), the content of naphthalene-sulfonate (~150 parts per million) is negligible. [b] Measured by organic elemental analysis. [c] Commercial grade pure PC from Teijin Co. Ltd. [d] Commercial grade PC-siloxane copolymer from SABIC Co. Ltd.

Subsequently, BPA, DPC, DN-SO_3Na, and DMS-Schiff were used to fabricate four different SS-co-PCs with varying polysiloxane block contents by transesterification and melt polycondensation (Fig. 1). Commercial pure PC (K-1300, Teijin Japan) and PC-siloxane copolymer (EXL9330, SABIC) were employed as reference specimens. The ^{13}C-NMR spectra of these copolymers are shown in Fig. 2(b). The chemical shifts at 1.07 and 30.98 ppm correspond to the carbon atoms in methyl of –Si–CH_3 and –C–CH_3, respectively, and that at 42.62 ppm represents the quaternary carbon in the PC chains. The signal at 152.20 ppm corresponds to the –C=O carbonyl group and those (d–g) reflect the multiplet splitting characteristic of aromatic carbons from BPA and the sulfonated naphthalene structures [38, 39]. By using peak (a) and peak (b) as standard peaks for the polysiloxane and PC blocks, respectively, and disregarding the negligible amount of DN-SO_3Na units, the polysiloxane block content in each copolymer, as well as EXL9330, can be determined via peak area ratio (Table 1). The polysiloxane block content in SS-co-PC5, SS-co-PC9, EXL9330, SS-co-PC14, and SS-co-PC20 was 5.02%, 9.26%, 11.27%, 14.31%, and 20.28%, respectively. FT-IR analysis was performed on SS-co-PC9 and pure PC (K-1300) (Fig. 2(c)). The characteristic peaks of K-1300 appear at 2975–2865 cm^{-1} (C–H of methyl or methylene groups), 1776–1723 cm^{-1} (C=O of carbonate groups), 1195 cm^{-1} (CH_3–C–CH_3 of isopropyl groups), 1017 cm^{-1} (C–C_{AR}), and 1236 and 889 cm^{-1} (carbonates) [40]. The FT-IR spectrum of SS-co-PC9 exhibits the characteristic peaks of both pure PC and DMS-Schiff. Additionally, a distinctive peak at 1171 cm^{-1}, corresponding to the S=O bond of the sulfonate group [8, 35], can be observed. These results confirm the successful incorporation of both DMS-Schiff blocks and DN-SO_3Na units into the PC polymer chain. The GPC results (Table 1) exhibit that as the polysiloxane block content increases, the M_n and M_w of SS-co-PCs increase, and the

molecular weight distribution narrows progressively. Compared to the commercial product EXL9330 from SABIC, the copolycarbonates fabricated in this work exhibit higher molecular weights and degrees of polymerization, albeit with slightly broader molecular weight distributions. This broader distribution may be attributed to factors such as the Schiff-base side groups and the sulfonated-naphthalene units in the backbone [41, 42].

Fig. 2(d–i) provides the transmission electron microscopy (TEM) images and averaged domain sizes (d_n) of SS-co-PCs, K-1300, and EXL9330. The copolycarbonates (SS-co-PCs and EXL9330) exhibit a typical sea-island morphology, where the darker dispersed phase corresponds to the polysiloxane blocks, and the lighter continuous phase represents the polycarbonate matrix. In SS-co-PC5 and SS-co-PC9, the domain size (d_n) of the polysiloxane phase is roughly similar, both below 50 nm. However, the dispersed phase of SS-co-PC9 is more uniform in size and densely distributed. When the proportion of the polysiloxane block increases to 14%, the domain size of the dispersed phase in SS-co-PC14 significantly increases, with an average d_n reaching 61.3 nm. Moreover, the average d_n of the dispersed phase in SS-co-PC20 further boosts to 65.9 nm. Obviously, as the content of polysiloxane blocks increases, the d_n gradually grows as well. Moreover, in certain regions of SS-co-PC9, SS-co-PC14, and SS-co-PC20, the distinct crystalline particles with a higher contrast can be observed (Fig. S1 in Supplementary Information), probably because of the crystallized naphthalene-sulfonate salts formed at low concentrations, with particle sizes ranging from 5 to 15 nm and content of 100–200 part per million approximately (based on the element analysis in Table 1). Fig. 2(j) presents the SAXS profiles of the (co)polycarbonate specimens, revealing that the polysiloxane phases in SS-co-PCs are not randomly or chaotically dispersed. Instead, they display a certain degree of ordered aggregation and stacking [43]. A broad primary scattering peak appears at the scattering

vector q_1 of 0.267 nm^{-1}, followed by secondary and tertiary scattering peaks with lower intensities at $\sqrt{7}q_1$ and $\sqrt{9}q_1$, respectively. This suggests that the dispersed polysiloxane phase forms a hexagonal close-packed cylindrical microstructure within the continuous PC phases [44]. In contrast, EXL9330 only exhibits the primary scattering peak (q_1) without the higher-order characteristic peaks, indicating that the polysiloxane blocks are randomly and uniformly dispersed within the PC matrix [45]. Compared to EXL9330, the more ordered aggregation of the polysiloxane phases in SS-co-PCs is conducive to reducing their sizes to a certain extent. Besides, as exhibited in viscosity (η^*)-frequency (ω) curves under a processing temperature of 225 °C (Fig. 2(k)), another principle for the improvement in microphase separation can be revealed clearly. In comparison with K-1300 and EXL9330, the naphthalene-sulfonate unit in SS-co-PCs catalyzes the degradation of PC chains (plasticizing effect) [5], which sharply reduces the melting-viscosity of the system and reforms the dispersion and morphology of polysiloxane regions. Additionally, the morphology tends to be more regular and spherical (consistent with the previously mentioned TEM images and the averaged domain size), which facilitates the transmission of visible lights and dissipates impact energy (under external forces).

3.2. Optical transparency of SS-co-PCs

The transparency of PC is crucial for its applications in architectural aesthetics, optical components, surgical instruments, etc. Although pure PC exhibits outstanding transparency (e.g., a PC film with a thickness of 0.3 mm achieving a visible-light transmittance of 90.2% and a haze of 1.8%), it often fails to meet stringent requirements such as high impact resistance, flame retardancy, low smoke emission, high flowability, and thermo-stability. Thus, the silicon-copolymerized polycarbonates have rapidly developed. As stated in Introduction, the commercial (co)-PC products exhibit various performance enhancements, but none have achieved

satisfactory transparency. The fundamental reason lies in the improper regulation of the phase behaviors of the polysiloxane phases.

Based on the TEM images, SAXS spectra, and rheology test ($\eta^*-\omega$ curves) in Fig. 2, we performed a detailed analysis of the microphase separation and domain sizes of the copolycarbonates. As shown in Fig. 3(a, b), even for materials with a higher polysiloxane block content (SS-co-PC14 and SS-co-PC20), the domain sizes of the dispersed phases are still smaller than those of EXL9330 with only 11% polysiloxane blocks. Within the range of visible light (400–800 nm), their optical transmittance remains above 80%, although the haze is significantly higher than that of pure PC. For SS-co-PC5 and SS-co-PC9, their optical transmittance approaches 90%, and their haze values are as low as 2.4% and 3.4%, respectively, which are comparable to those of pure PC (K-1300). This can be attributed to the relatively regular stacking and aggregation of their dispersed phases, reduction in viscosity of PC matrix (i.e., smaller and more uniform domain sizes), and lower content of polysiloxane blocks. The transparency of these films is clearly illustrated in Fig. 3(c).

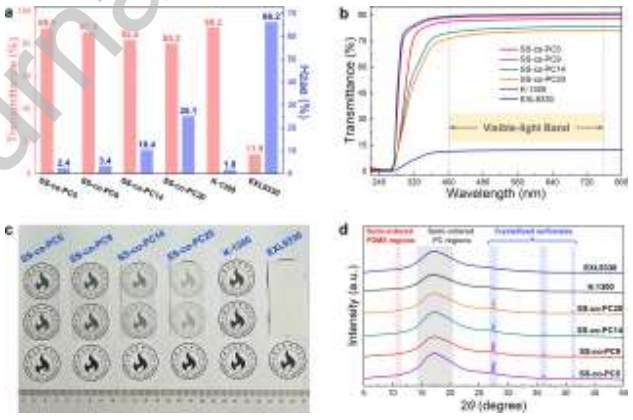

Fig. 3. The (a) transmittance and haze, (b) UV-Vis spectra between the wavelength from 200 to 800 nm, (c) digital photos, and (d) XRD patterns of SS-co-PCs, K-1300 and EXL9330 films (thickness: 0.3 mm).

Moreover, Fig. 3(d) presents the X-ray diffraction (XRD) patterns of SS-co-PCs, EXL9330, and K-1300. The broad peak near 2θ of ~17.3° corresponds to the semi-crystalline regions of the PC blocks, reflecting the characteristic short-range order and long-range disorder of the glassy state [6, 8]. Therefore, pure PC, such as K-1300, is a glassy polymer with low crystallinity, leading to its excellent transparency. For SS-co-PCs and EXL9330, the semi-crystalline features of the PDMS blocks appear at 2θ of ~11.5° and ~20.0° (overlapping with the broad peak of PC) [46, 47]. However, no significant enhancement in PC crystallinity is observed, suggesting that the transparency differences between SS-co-PCs and EXL9330 are not related to their crystallization behaviors. Instead, the varying degrees of microphase separation and the resulting light scattering, caused by differences in molecular chain flexibility and refractive indices between PDMS and PC, are the primary factors affecting the transmittance and haze of these copolycarbonates. In summary, compared to EXL9330, through better regulation of the dispersed-phase behaviors, SS-co-PCs achieve both high transparency and low haze at a lower polysiloxane block content, minimizing the adverse effects of increased light scattering due to the microphase separation and uneven arrangement of rigid PC chains and flexible PDMS blocks.

3.3. Fire safety and mechanical behaviors of SS-co-PCs

Fire safety and mechanical performance are the core criteria for PC as an engineering plastic, and many modification studies are based on these aspects [48–52]. Fig. 4(a–c) presents the results of cone calorimetry (heat release rate and smoke release rate), limiting oxygen index (LOI), and vertical combustion (for 1.6 mm thick specimens) tests of SS-co-PCs, K-1300, and EXL9330. Detailed data are summarized in Table 2. For pure PC (K-1300), upon ignition, the peak heat release rate (PHRR) reaches 622.5 kW m^{-2} at 250 s, and the total heat release (THR, as calculated from the areas of HRR-t curves) reaches 133.2 MJ m^{-2}. The peak smoke production

rate (PSPR) is 0.277 $m^2 s^{-1}$, with a total smoke release (TSR, based on the integral areas of SPR-t curves) of 2686.2 $m^2 m^{-2}$. Overall, the combustion process of K-1300 is intense and rapid, with substantial toxic gas emissions, and flameout occurs around 320 s. When polysiloxane blocks and naphthalene-sulfonate groups are introduced into the copolymer, the fire behaviors of SS-co-PCs change dramatically. For SS-co-PC5, the hazards of heat radiation and smoke/toxic gas emission are significantly reduced. As the polysiloxane block content increases to 9%, 14%, and 20%, the PHRR and PSPR of SS-co-PCs gradually decrease. Based on the HRR-t and SPR-t curves, SS-co-PC9 demonstrates a favorable flame-retardant performance, with PHRR and PSPR of 293.0 kW m^{-2} and 1601.8 $m^2 s^{-1}$, representing 53% and 85% reductions compared to those of K-1300. Additionally, SS-co-PC9, SS-co-PC14, and SS-co-PC20 exhibit a significant suppression in CO yield (COY), with decreases of about 30%–40% compared to K-1300. In contrast, EXL9330 (containing 11% polysiloxane blocks) shows a comparable heat release suppression to SS-co-PC5 and SS-co-PC9 but a lower smoke suppression efficiency. The higher flame-retardant efficiency of SS-co-PCs, despite SS-co-PCs and EXL9330 being polysiloxane-copolymerized PC resins, can be attributed to two factors: (1) the differences in dispersed phase behavior (SS-co-PCs with better microphase separation and aggregation structures), and (2) the synergistic flame-retardant effect of trace naphthalene-sulfonate units [53, 54].

We observed unexpected decreases in the residual chars (RCs) of SS-co-PCs and EXL9330 compared to K-1300, which contradicts the traditional correlation between flame-retardant performance and char yield. However, this phenomenon can be explained by the flame-retardant mechanisms reported for organosilicon and sulfonate-containing PC composite systems. Generally, the well-dispersed organosilicon tends to migrate to the polymer surface [55], ultimately forming lightweight, white particles embedded into the char layers (Fig. S2).

Meanwhile, the sulfonate system tends to enhance the crosslinking density of the PC char rather than increase its mass, promoting the release of vapor H_2O and CO_2 during the thermal degradation of PC, thereby diluting flammable gases such as phenol and methane [56].

Table 2 LOI, vertical combustion (UL-94) rating (thickness: 1.6 mm), and cone calorimetry data of SS-co-PCs and commercial samples.

Parameters	SS-co-PC5	SS-co-PC9	SS-co-PC14	SS-co-PC20	K-1300	EXL9330
UL-94 (1.6 mm)	V-1	V-0	V-0	V-0	V-2	V-1
LOI (%)	31.4 ± 0.2	32.4 ± 0.1	32.6 ± 0.1	34.5 ± 0.2	23.9± 0.1	28.4 ± 0.1
[a] TTI (s)	97 ± 2	90 ± 4	86 ± 3	82 ± 2	79 ± 2	78 ± 3
[a] PHRR (kW m^{-2})	377.5 ± 6.3	293.0 ± 7.5	273.5 ± 10.2	263.7 ± 5.9	622.5 ± 11.3	308.6 ± 8.7
[a] t-PHRR (s)	220 ± 5	260 ± 3	295 ± 5	345 ± 3	250 ± 3	250 ± 5
[a] THR (MJ m^{-2})	61.8 ± 6.4	68.7 ± 5.5	70.1 ± 9.2	73.6 ± 7.6	133.2 ± 4.9	72.1 ± 4.3
[a] FPI	0.257	0.307	0.314	0.315	0.127	0.253
[b] TSR (m^2 m^{-2})	1760.0 ± 15.6	1601.8 ± 23.1	1588.4 ±14.5	1425.6 ± 19.3	2686.2 ± 16.6	1901.1 ± 18.0
[b] PSPR (m^2 s^{-1})	0.15 ± 0.01	0.11 ± 0.00	0.09 ± 0.00	0.08 ± 0.01	0.28 ± 0.02	0.20 ± 0.02
[b] CO_2Y (kg kg^{-1})	1.56 ± 0.04	1.52 ± 0.05	1.51 ± 0.04	1.51 ± 0.03	1.59 ± 0.06	1.72 ± 0.05
[b] COY (kg kg^{-1})	0.09	0.08	0.08	0.07	0.12	0.10
[c] AMLR (g s^{-1})	0.054 ± 0.003	0.050 ± 0.004	0.046 ± 0.003	0.045 ± 0.003	0.075 ± 0.002	0.057 ± 0.002
[c] Chars (wt%)	9.5 ± 1.2	11.3 ± 0.8	13.0 ± 0.8	14.3 ± 0.5	16.7 ± 2.0	17.2 ± 1.7

[a] TTI, PHRR, t-PHRR, THR, and FPI refer to time-to-ignition, peak heat release rate, time to PHRR, total heat release, and fire performance index, respectively. [b] TSR, PSPR, CO_2Y, and COY represent the total smoke release, peak smoke production rate, and averaged CO_2 and CO yield, respectively. [c] AMLR and

Chars mean the average mass loss rate and yield of residual chars after cone calorimetry, respectively.

In industry, the LOI and vertical combustion ratings are the essential parameters to evaluate flame retardancy. For PC, achieving a UL-94 V-0 rating under a low thickness (≤ 1.6 mm) remains highly challenging. The unmodified K-1300 has an LOI of 23.9% and a UL-94 V-2 rating, indicating that it has char-formation ability but suffers from poor anti-dripping performance, which can easily cause a secondary ignition. SS-co-PC5 achieves a significantly increased LOI of 31.4%, but its UL-94 rating is V-1 under the thickness of 1.6 mm. As the polysiloxane block content increases to 9%, 14%, and 20%, the LOI of SS-co-PCs rises to 32.4%, 32.6%, and 34.5%, respectively. Notably, SS-co-PC9, SS-co-PC14, and SS-co-PC20 achieve a UL-94 V-0 rating with an obvious anti-dripping ability, demonstrating a significant breakthrough for thin-walled samples. EXL9330 exhibits an LOI of 28.4% and a UL-94 V-1 classification, slightly inferior to SS-co-PC5. Furthermore, the fire performance index (FPI), which is the ratio of time-to-ignition (TTI) to PHRR, is commonly used to assess the fire propagation and growth potential of polymers. A higher FPI indicates better fire safety. K-1300 has a TTI of only 79 s and a relatively high PHRR, resulting in an FPI of only 0.127 (m^2 s) kW^{-1}. In contrast, the SS-co-PCs and EXL9330 samples show significant improvements in FPI. In particular, the SS-co-PC9, SS-co-PC14, and SS-co-PC20 samples achieve UL-94 V-0 ratings with FPIs exceeding 0.3 (m^2 s) kW^{-1}, demonstrating their superior fire retardancy.

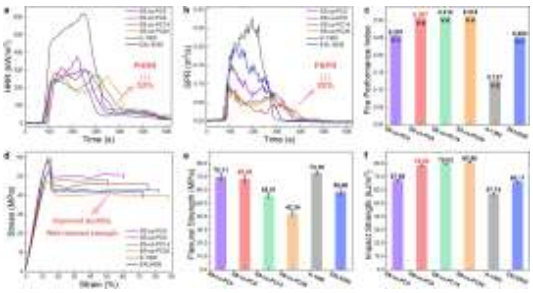

Fig. 4. (a) HRR and (b) SPR versus time curves, (c) fire performance index (FPI), (d) tensile stress-strain curves, and (e) flexural and (f) impact strength of SS-co-PCs, K-1300 and EXL9330.

Fig. 4(d–f) illustrates the mechanical properties (tensile, flexural, and impact performances) of SS-co-PCs, K-1300, and EXL9330. Bulk PC (K-1300) exhibits a high tensile strength of approximately 60.0 MPa and an elongation at a break of 50.8%. Its flexural strength and impact strength are 73.16 MPa and 57.15 kJ m^{-2}, respectively. Although superior to general plastics in terms of strength and toughness, further improvement in impact resistance and ductility is necessary for high-end engineering applications. With the incorporation of just 5% polysiloxane blocks, SS-co-PC5 shows notable improvements in mechanical performances, with an elongation at break increasing to 60.4% and an impact strength reaching 67.60 kJ m^{-2}, representing enhancements of 12% and 18% compared to those of K-1300. Simultaneously, it retains comparable tensile strength (58.7 MPa) and flexural strength (70.11 MPa) to pure PC. These results suggest that the introduction of elastomeric blocks significantly enhances the impact resistance and tensile ductility of PC, but does not impair the mechanical strength. As the polysiloxane block content increases, the elongation at break and impact strength of SS-co-PC9, SS-co-PC14, and SS-co-PC20 progressively improve. Among them, SS-co-PC9 exhibits the best performance portfolio, considering transparency and flame retardancy. Its elongation at break and impact strength reaches 75.4% and 78.83 kJ m^{-2}, with 48% and 38% increases compared to pure PC, and surpasses those of EXL9330. However, with increasing polysiloxane content, the tensile strength and flexural strength of SS-co-PCs gradually decline. For SS-co-PC9, the tensile strength and flexural strength are maintained at 57.2 and 68.48 MPa, respectively, with reductions of less than 7% compared to K-1300. When the polysiloxane content is further

increased to 14% and 20%, the mechanical strength decreases more significantly, displaying the typical characteristics of an elastomer with a "soft yet tough" behavior. The impressive elongation at break and impact toughness of the SS-co-PCs can be attributed to the unique properties of polysiloxane and sulfonate units. The polysiloxane blocks, with their flexible Si-O backbone, contribute to the increased chain mobility and energy dissipation capacity of the polymer chains. This enhanced flexibility allows the polymer to deform more readily under stress, leading to a higher elongation at break. Additionally, the polysiloxane blocks can act as physical cross-linkers, further improving the toughness of the copolymers. Besides, thanks to the naphthalene-sulfonate units, the processing viscosity was reduced obviously thus promoting the microphase behaviors. The well-controlled phase separation of the polysiloxane blocks within the polycarbonate matrix is crucial for the mechanical performance.

In summary, SS-co-PC9 achieves an optimal balance between transparency, fire safety, mechanical strength, and impact toughness. It retains the valuable characteristics of pure PC, such as high optical transmittance, low haze, and excellent mechanical strength, while achieving the stringent UL-94 V-0 rating (1.6 mm) with an LOI of 32.4%, and significantly reduced PHRR and PSPR. Notably, its notched impact strength reaches nearly 79 kJ m^{-2}. SS-co-PC9 with such a high-performance portfolio can find ubiquitous applications in various industries.

3.4. Toughening and flame-retardant mechanisms

As shown in Fig. 5, in order to further elucidate the superior impact resistance of SS-co-PCs, their fractured surface morphologies after impact failure were studied by scanning electron microscopy (SEM) [57–59] and compared with those of K-1300 and EXL9330. K-1300 reveals a relatively smooth and flat fractured surface. Despite a certain degree of toughness, under high-frequency (high-rate) impact, the relatively rigid chains of PC undergo a ductile-to-brittle

transition, failing to sufficiently dissipate momentary energy, thus exhibiting a typical brittle rupture pattern. In contrast, EXL9330 shows a more undulating and rough surface, with large tear-like cavities, indicative of a classic ductile fracture, further demonstrating the increased impact strength. The SS-co-PCs, however, exhibit two distinct morphological features on their fractured surfaces, which is an uncommon phenomenon in PC composite systems during impact failure, providing insight into their ultrahigh impact strength. In the first stage (Fig. 5(a–c)), the area near the notch is characterized by densely distributed fine cavities with varying depths, resembling elastomeric particles being forcibly pulled out of the matrix, indicative of the strong interfacial bonding between polycarbonate and polysiloxane phases. In the second stage (Fig. 5(a_1–c_1)), compared to EXL9330, the fractured surface becomes more rugged, twisted, and wrinkled, with even burrs and thin fibers/filaments generated, indicating a rapid polymer chain response and deformation during impact.

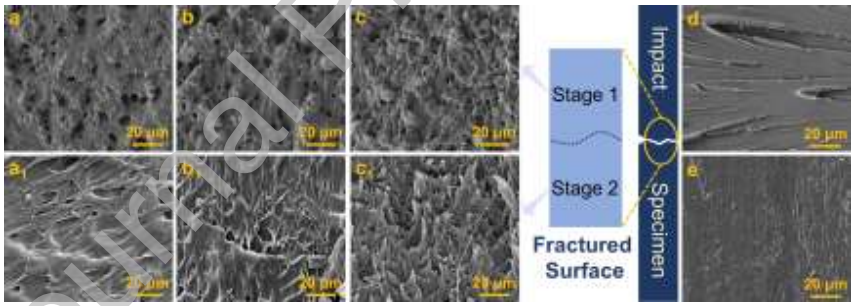

Fig. 5. SEM images of impact-failure fractured interfaces for (a) SS-co-PC5, (b) SS-co-PC9, (c) SS-co-PC14, (d) K-1300, and (e) EXL9330. Among them, SS-co-PCs exhibited two types of fractured micro-morphologies.

When SS-co-PCs are subjected to high-frequency impacts, the elastomeric blocks undergo microphase separation, harden and are forcibly pulled out of the continuous PC phases. However, the smaller and more uniformly dispersed polysiloxane domains are capable of absorbing more impact energy. Consequently, the first stage of the surface fracture shows more pronounced

ductile tearing yet rough characteristics. After a brief macromolecular chain relaxation, the materials can rapidly deform in the second stage, dissipating more energy. Therefore, the materials fail in a relatively ductile state, and some of them even display “fibrillation” in their cross-sections, where elongated fibers or filaments are pulled out.

Fig. 6(a–e) shows the SEM images of the external surface for residual chars after the cone calorimetric tests, as well as the energy-dispersive spectroscopy (EDS) mappings of Si and S elements. The residual char layer of pure PC (K-1300) exhibits a loose and porous morphology at the microscopic scale, with a tendency towards powdering. This fragile char layer, with pores and defects, is highly disadvantageous for inhibiting heat radiation, smoke release, and blocking heat and mass exchange [60]. Consequently, K-1300 underwent intense combustion during the cone calorimeter test, releasing large amounts of black and toxic smoke, and it also suffered from poor performances in vertical combustion and LOI tests.

In comparison, the SEM images of the char residues of SS-co-PCs reveal that, under the combined effects of naphthalene-sulfonate units and polysiloxane blocks, the char surface becomes progressively smoother, denser, and more continuous as the polysiloxane block content increases. Notably, the completeness of the EXL9330 char lies between those of SS-co-PC5 and SS-co-PC9, which correlates with the enhancement in flame retardancy. Furthermore, EDS results indicate that the Si and/or S elements are uniformly distributed and embedded in the condensed phase, suggesting that the well-dispersed flame retardant system exerts a significant catalytic effect on charring during combustion.

To further explore potential gas-phase flame retardant mechanisms, Fig. 6(f, g) displays the 3D TG-IR profiles of K-1300 and SS-co-PC9 under air atmosphere. Compared to K-1300, SS-co-PC9 demonstrates a significantly reduced release of degradation products (as evidenced by the

decreased IR peak intensity), corresponding to the reduction in average heat release rate (AMLR) obtained from cone calorimetry. However, the composition of the degradation products between these two polymers is almost identical, suggesting that the gas-phase effects of the polysiloxane and naphthalene-sulfonate parts are not obvious. Therefore, the flame-retardant mechanism of the siloxane and sulfonate systems in PC is primarily reflected in the condensed phase, characterized by catalytic charring, surface coverage, and heat-mass shielding [61–66].

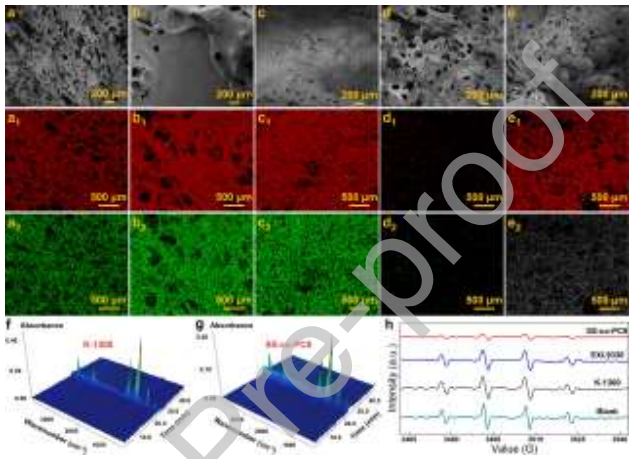

Fig. 6. SEM images, EDS mappings (Si for red and S for green) of the external surface of residual chars after cone calorimetry for (a) SS-co-PC5, (b) SS-co-PC9, (c) SS-co-PC14, (d) K-1300, and (e) EXL9330. (f, g) 3D TG-IR spectra (under air atmosphere) and (h) ESR intensity curves of K-1300, EXL9330, and SS-co-PC9.

It can be concluded that although the polysiloxane and naphthalene-sulfonate components enhance the char quality, they do not increase the char yield and have little gas-phase action. Therefore, the free radical scavenging effect should be considered [12]. Hydroxyl radicals (HO•) are highly reactive species that can trigger chain-thermal degradation in polymers, making them appropriate targets to evaluate the radical suppression effects of SS-co-PCs. HO• are typically generated via the Fenton reaction ($H_2O_2 + Fe^{2+} \rightarrow HO\bullet + Fe^{3+} + OH^-$) and subsequently captured by the spin-trapping agent DMPO, forming a stable complex that can be quantitatively detected

through electron spin resonance (ESR) [8]. Fig. 6(h) presents the ESR spectra of K-1300, EXL9330, and SS-co-PC9. Since the materials do not decompose at room temperature (and cannot be dissolved in buffer solution), they were hydrolyzed under alkaline conditions for a period of time [67]. In the blank control-group, the curve shows the characteristic 1:2:2:1 quadruplet-peaks for HO•, with no significant change in ESR signal intensity after the addition of 2.5 mg of hydrolyzed K-1300 or EXL9330. This indicates that neither pure PC nor polysiloxane-copolymerized PC after degradation can capture HO• in the system, confirming the absence of a notable radical trapping effect for the polysiloxane system. However, after the addition of an equivalent amount of hydrolyzed product for SS-co-PC9, the intensity of the HO• characteristic peaks significantly decrease. This demonstrates that the naphthalene-sulfonate units possess a radical trapping ability, which is one of the key reasons why the SS-co-PC system exhibits superior flame retardancy relative to EXL9330 in addition to the more effective dispersion behavior of the polysiloxane phase.

4. Conclusions

In this work, we successfully developed a series of poly(carbonates-b-siloxanes) with intrinsic flame-retardant and impact-resistant properties through the incorporation of Schiff-base modified polysiloxanes and naphthalene-sulfonate units into the polycarbonate chains. The optimal balance between optical property, fire safety, and mechanical performance was realized in SS-co-PC9, which exhibited superior flame retardancy, transparency, and impact toughness, and maintained excellent tensile and flexural strength. The synergistic flame-retardant effects of the naphthalene-sulfonate and polysiloxane units and the well-controlled dispersion of the polysiloxane blocks play critical roles in enhancing the overall performances of these copolymers. These results demonstrate the potential of SS-co-PCs in high-end applications,

providing a robust theoretical foundation for the future design of advanced flame-retardant polycarbonates.

Acknowledgments

This work was financially supported by the National Natural Science Foundation of China (No. 52403117, 52173083, 51991355, and 52173082), the 2024 Ningbo Yongjiang Talent Programme, the Natural Science Foundation of Zhejiang Province (No. LY24E030007), and the Australian Research Council (No. DE230100616).

References

[1] D. Kyriacos, Polycarbonates, Brydson's Plastics Materials, Elsevier, Amsterdam, 2017, pp. 457–485.

[2] X. Mu, Z. Jin, F. Chu, W. Cai, Y. Zhu, B. Yu, L. Song, Y. Hu, Compos. Part B-Eng. 238 (2022) 109873.

[3] Z. Liu, M. Ma, B. Ge, Y. Zheng, S. Chen, Y. Shi, H. He, Y. Zhu, X. Wang, Chem. Eng. J. 474 (2023) 145799.

[4] X.X. Xiao, Q. Zhang, T.Y. Bai, Z.X. Chen, Z.N. Wang, J.H. Bai, L. Chen, B.W. Liu, Y.Z. Wang, Small (2024) 2401429. DOI: 10.1002/smll.202401429.

[5] S.V. Levchik, E.D. Weil, Polym. Int. 54 (2005) 981–998.

[6] T. Sai, S. Ran, Z. Guo, H. Yan, Y. Zhang, H. Wang, P. Song, Z. Fang, Chem. Eng. J. 409 (2021) 128223.

[7] Z.X. Chen, Z.Y. Zhao, P. Lu, X.X. Xiao, S. He, C. Deng, Y.Z. Wang, ACS Appl. Polym. Mater. 5 (2023) 4889–4900.

[8] T. Sai, S. Ran, S. Huo, Z. Guo, P. Song, Z. Fang, Chem. Eng. J. 433 (2022) 133264.

[9] S.V. Levchik, E.D. Weil, J. Fire Sci. 24 (2006) 137–151.

[10] L. Chen, Y.Z. Wang, Polym. Adv. Technol. 21 (2010) 1–26.

[11] A.B. Morgan, J.W. Gilman, Fire Mater. 37 (2013) 259–279.

[12] T. Sai, S. Ran, Z. Guo, P. Song, Z. Fang, SusMat 2 (2022) 411–434.

[13] B.W. Liu, H.B. Zhao, Y.Z. Wang, Adv. Mater. 34 (2022) 2107905.

[14] Q. Chen, T. Sai, Z. Fang, Z. Guo, J. Therm. Anal. Calorim. 146 (2021) 1383–1392.

[15] X. Huang, X. Ouyang, F. Ning, J. Wang, Polym. Degrad. Stabil. 91 (2006) 606–613.

[16] H. Nishihara, Y. Suda, T. Sakuma, J. Fire Sci. 21 (2003) 451–464.

[17] J.M. Goossens, B.P. Hendrix, W. van der Heijden, C.J. Maas, H. Verhoogt, Transparent, fire-resistant polycarbonate, US Patent, No. 20020723703, 2004.

[18] H. Hu, L. Wang, L. Wang, L. Li, S. Feng, Polym. Chem. 11 (2020) 7721–7728.

[19] Y. Zhu, R. Yu, S. Wang, H. Xing, J. Qiu, J. Liu, T. Tang, Chem. Eng. J. 446 (2022) 136742.

[20] S. Wang, X. Yang, Z. Li, X. Xu, H. Liu, D. Wang, H. Min, S. Shang, Compos. Sci. Technol. 198 (2020) 108272.

[21] Y.L. Tang, G.Q. Zheng, Y.X. Lin, P. Lu, H.B. Zhao, D.M. Guo, L. Chen, B.W. Liu, Y.Z. Wang, Polym. Degrad. Stabil. 214 (2023) 110416.

[22] M. Jiang, B.W. Liu, F.M. He, Q. Zhang, A. Wang, D.M. Guo, H.B. Zhao, L. Chen, Y.Z. Wang, Chem. Eng. J. 455 (2023) 140637.

[23] S.Y. Zhang, T. Fu, Y. Gong, D.-M. Guo, X.L. Wang, Y.Z. Wang, Chinese Chem. Lett. 34 (2023) 107615.

[24] B.W. Liu, H.B. Zhao, L. Chen, L. Chen, X.L. Wang, Y.Z. Wang, Compos. Part B-Eng. 211 (2021) 108664.

[25] B.W. Liu, L. Chen, D.M. Guo, X.F. Liu, Y.F. Lei, X.M. Ding, Y.Z. Wang, Angew. Chem. Int. Edit. 58 (2019) 9188–9193.

[26] B.W. Liu, Y.F. Lei, X.F. Liu, D.M. Guo, L. Chen, Y.Z. Wang, Polymer 218 (2021) 123430.

[27] D.J. Liaw, P. Chang, Polymer 38 (1997) 5545–5550.

[28] S. Salhofer, B. Steuer, R. Ramusch, P. Beigl, Waste Manage. 57 (2016) 27–35.

[29] E. Directive, Off. J. Eur. Communities 46 (2013) 19–23.

[30] R. Kambour, H. Klopfer, S. Smith, J. Appl. Polym. Sci. 26 (1981) 847–859.

[31] A. Nodera, T. Kanai, J. Appl. Polym. Sci. 100 (2006) 565–575.

[32] M.I. Mollah, D.W. Seo, M.M. Islam, Y.D. Lim, S.H. Cho, K.M. Shin, J.H. Kim, W.G. Kim, J. Macromol. Sci. A 48 (2011) 400–408.

[33] M.M. Islam, D.W. Seo, H.H. Jang, Y.D. Lim, K.M. Shin, W.G. Kim, Macromol. Res. 19 (2011) 1278–1286.

[34] H.A. van Aert, L. Nelissen, P.J. Lemstra, D.J. Brunelle, Polymer 42 (2001) 1781–1788.

[35] Z.X. Chen, Z.Y. Zhao, P. Lu, X.X. Xiao, S. He, C. Deng, Y.Z. Wang, Polym. Degrad. Stabil. 214 (2023) 110388.

[36] X. Wang, L. Wang, X. Fan, J. Guo, L. Li, S. Feng, Polymer 229 (2021) 124021.

[37] J.H. Gao, B. Wan, M.-S. Zheng, L. Luo, H. Zhang, Q.L. Zhao, G. Chen, J.W. Zha, Mater. Horiz. 11 (2024) 1305–1314.

[38] E. Williams, J. Cargioli, S. Hobbs, Macromolecules 10 (1977) 782–785.

[39] Y. Han, Y. Zhang, X. Long, W. Bai, Q. Wang, G. Wang, J. Appl. Polym. Sci. 141 (2024) e54770.

[40] T. Sai, Y. Su, H. Shen, S. Ran, S. Huo, Z. Guo, Z. Fang, ACS Appl. Mater. Interfaces 13 (2021) 30061–30075.

[41] D.T. Gentekos, J. Jia, E.S. Tirado, K.P. Barteau, D.M. Smilgies, R.A. DiStasio Jr, B.P. Fors, J. Am. Chem. Soc. 140 (2018) 4639–4648.

[42] S. Song, H. Zhou, I. Manners, M.A. Winnik, Chem 7 (2021) 2800–2821.

[43] R. Yadav, M. Naebe, X. Wang, B. Kandasubramanian, Sci. Rep. 7 (2017) 7706.

[44] M.D. Ninago, A.J. Satti, A.E. Ciolino, E.M. Vallés, M.A. Villar, D.A. Vega, A. Sanz, A. Nogales, D.R. Rueda, J. Polym. Sci. Pol. Chem. 48 (2010) 3119–3127.

[45] Y.L. Qin, P. Zhu, C.X. Ouyang, X. Dong, Chinese J. Polym. Sci. 42 (2024) 87–96.

[46] G.L. Jadav, V.K. Aswal, H. Bhatt, J.C. Chaudhari, P.S. Singh, J. Membrane Sci. 415 (2012) 624–634.

[47] A. Cordoba, E.M. Rivera-Muñoz, R. Velázquez-Castillo, K. Esquivel, Nanomaterials 13 (2023) 1699.

[48] Z. Zhao, Z. Zhang, C. Sun, M. Xu, B. Li, Polym. Degrad. Stabil. 220 (2024) 110648.

[49] J. Zhang, J. Liu, J. Sun, X. Liu, H. Li, X. Gu, J. Zhao, S. Zhang, Prog. Org. Coat. 186 (2024) 108022.

[50] Z.T. Xiao, Y. Hu, A. Mohammdi, X. Wang, Chem. Eng. J. 499 (2024) 156499.

[51] N. Li, Y. Li, Y. Zhu, J. Zhang, J. Liu, Z. Jiang, M. Li, T. Tang, Compos. Part A-Appl. Sci. Manuf. 186 (2024) 108432.

[52] X. Ye, C. Zhan, B. Wang, T. Sai, C. Zhang, J. Li, Z. Guo, S. Huo, Polym. Degrad. Stabil. 230 (2024) 111012.

[53] D. Yuan, H. Yin, X. Cai, J. Therm. Anal. Calorim. 114 (2013) 19–25.

[54] Y. Feng, S. Zhong, X. Cui, Y. Li, C. Ding, L. Cui, M. Wang, Y. Yang, W. Liu, Electrochim. Acta 379 (2021) 138113.

[55] W. Zhang, G. Camino, R. Yang, Prog. Polym. Sci. 67 (2017) 77–125.

[56] Y.Z. Wang, B. Yi, B. Wu, B. Yang, Y. Liu, J. Appl. Polym. Sci. 89 (2003) 882–889.

[57] G. Ye, S. Huo, C. Wang, Q. Zhang, H. Wang, P. Song, Z. Liu, Small 20 (2024) 2404634.

[58] Y. Xue, M. Zhang, S. Huo, Z. Ma, M. Lynch, B.T. Tuten, Z. Sun, W. Zheng, Y. Zhou, P. Song, Adv. Fun. Mater. 34 (2024) 2409139.

[59] J. Feng, Y. Sun, P. Song, W. Lei, Q. Wu, L. Liu, Y. Yu, H. Wang, ACS Sustainable Chem. Eng. 5 (2017) 7894–7904.

[60] T. Sai, S. Ran, Z. Guo, H. Yan, Y. Zhang, P. Song, T. Zhang, H. Wang, Z. Fang, Compos. Part B-Eng. 197 (2020) 108064.

[61] H. Wang, S. Huo, C. Wang, G. Ye, Q. Zhang, P. Song, H. Wang, Z. Liu, Prog. Org. Coat. 193 (2024) 108562.

[62] T. Sai, S. Ran, Z. Guo, Z. Fang, Compos. Part B-Eng. 176 (2019) 107198.

[63] W. Yang, Q. Zhou, W. Pan, S. Zhu, C. Wei, H. Lu, W. Yang, A.C. Yuen, Chem. Eng. J. 469 (2023) 143935.

[64] Y. Xu, W.J. Yang, Q.K. Zhou, T.Y. Gao, G.M. Xu, Q.L. Tai, S.E. Zhu, H.D. Lu, R.K. Yuen, W. Yang, C.X. Wei, Chem. Eng. J. 450 (2022) 138475.

[65] C. Wang, S. Huo, G. Ye, Q. Zhang, C.F. Cao, M. Lynch, H. Wang, P. Song, Z. Liu, Chem. Eng. J. 500 (2024) 157418..

[66] J. Wang, J. Wang, S. Yang, X. Chen, K. Chen, G. Zhou, X. Liu, L. Xu, S. Huo, P. Song, H. Wang, Chem. Eng. J. 485 (2024) 149852.

[67] F.S. Liu, Z. Li, S.T. Yu, X. Cui, C.X. Xie, X.P. Ge, J. Polym. Environ. 17 (2009) 208–211.

Graphical abstract

Declaration of interests

☒ The authors declare that they have no known competing financial interests or personal relationships that could have appeared to influence the work reported in this paper.

☐The authors declare the following financial interests/personal relationships which may be considered as potential competing interests: